

This is the Appendix to the second of a three-paper investigation into valve spring design for race engines. The authors are **Gordon P. Blair, CBE, FREng** of Prof. Blair & Associates, **Charles D. McCartan, MEng, PhD** of the Queen's University Belfast and **W. Melvin Cahoon, BSc** of Volvo Penta of the Americas

Tapered valve spring design principles

In the Second Paper of this trilogy of papers on valve spring design for race engines ('Taper Design', published in Race Engine Technology issue 036), we examined in detail the design of three tapered valve springs; (a) and (b) round wire springs from two (speedway racing) motorcycle engines and (c) an ovate wire spring from a large capacity v-twin motorcycle power unit. Such was the complexity of the spring characteristics emanating from these few examples that, finding no design guidance in the literature and, empowered by the accuracy of our modelling [1.4] of all twelve valve springs in all three Papers of this study, we decided to use these spring modelling techniques in order to provide the designer with an Appendix exclusively devoted to the design of tapered valve springs.

THE VALVE SPRING DESIGNS STUDIED IN THIS APPENDIX

There are eleven tapered valve spring designs studied in this Appendix to Paper Two. The physical geometry of all eleven springs, using the nomenclature of Figs.2.2, 2.4 and 2.6, are presented in Fig.A1. In this

Paper Two Appendix, the Figures are conventionally labelled as Fig.A1 to Fig.A30. Any Figure from other parts of the trilogy can be referred to very simply; for example the Figs.2.2, 2.4 and 2.6 referred to above are originally presented as Figs.2, 4 and 6 in Paper Two. A similar rule applies to any previous References cited; new References cited within this Appendix are listed as A1 to A3.

THE VALVE SPRINGS IN THIS PAPER TWO APPENDIX

In Fig.A1 is a table giving the physical dimensions of all of the valve springs. The basic data of free spring height (Hucs), wire diameter (Ts), and the outside diameter (Ds) are kept constant; the final spring E1 has one physical dimension as an exception. The valve springs are labelled in sets and the colour banding of sections of the data for either the coil spaces P or the spring tapers D indicate the use of common numbers.

The first A set is A0 to A0.3 where the spring has equal spaces P and simple tapers D varying from zero to 0.3 mm per coil in equal increments; that makes spring A0 a plain parallel spring and is clearly used as a base reference for the spring characteristics of the other

tapered springs.

The second set is B1 and B2 where the coil spaces P are common with the A set but the taper D is in two segments.

The third set is C1 and C2 where the taper D is in two segments and identical with the B set, but the coil spaces P introduce progression to the C springs.

The fourth set is D1 and D2 where the taper D is identical with the A set but the coil spaces P are identical to the C springs.

The final demonstration spring E1 has the coil taper of spring D2 and very similar progression to a D spring, but it uses a minor change to its outside diameter Ds.

Fig.A1 Geometry of the test valve springs; series A and B.

NAME OF TAPERED SPRING	A0	A0.1	A0.2	A0.3	B1	B2
number of coils Sc	7	7	7	7	7	7
calculated mass of spring Ms (g)	53.3	51.9	50.5	49.1	50.7	50.6
free spring height Hucs (mm)	50	50	50	50	50	50
spring outside diameter Ds (mm)	30	30	30	30	30	30
spring wire diameter Ts (mm)	4	4	4	4	4	4
calculated free spring stiffness k (N/mm)	28.2	30.4	33.2	36.1	31.7	30.6
TAPER OF THE VALVE SPRING COILS						
side clearance D1 (mm)	0	0.6	1.2	1.8	1.8	1.2
side clearance D2 (mm)	0	0.5	1	1.5	1.2	0.8
side clearance D3 (mm)	0	0.4	0.8	1.2	0.6	0.4
side clearance D4 (mm)	0	0.3	0.6	0.9	0	0
side clearance D5 (mm)	0	0.2	0.4	0.6	0	0
side clearance D6 (mm)	0	0.1	0.2	0.3	0	0
side clearance D7 (mm)	0	0	0	0	0	0
SPACING OF THE VALVE SPRING COILS						
coil space P1 (mm)	4.6	4.6	4.6	4.6	4.6	4.6
coil space P2 (mm)	4.6	4.6	4.6	4.6	4.6	4.6
coil space P3 (mm)	4.6	4.6	4.6	4.6	4.6	4.6
coil space P4 (mm)	4.6	4.6	4.6	4.6	4.6	4.6
coil space P5 (mm)	4.6	4.6	4.6	4.6	4.6	4.6

NAME OF TAPERED SPRING	C1	C2	D1	D2	E1
number of coils Sc	7	7	7	7	7
calculated mass of spring Ms (g)	50.6	51.4	49	50.4	50.4
free spring height Hucs (mm)	50	50	50	50	50
spring outside diameter Ds (mm)	30	30	30	30	31
spring wire diameter Ts (mm)	4	4	4	4	4
calculated free spring stiffness k (N/mm)	31.7	30.5	35.1	33.2	33.2
TAPER OF THE VALVE SPRING COILS					
side clearance D1 (mm)	1.8	1.2	1.8	1.2	1.2
side clearance D2 (mm)	1.2	0.8	1.5	1	1
side clearance D3 (mm)	0.6	0.4	1.2	0.8	0.8
side clearance D4 (mm)	0	0	0.9	0.6	0.6
side clearance D5 (mm)	0	0	0.6	0.4	0.4
side clearance D6 (mm)	0	0	0.3	0.2	0.2
side clearance D7 (mm)	0	0	0	0	0
SPACING OF THE VALVE SPRING COILS					
coil space P1 (mm)	5.9	5.9	5.9	5.9	5.5
coil space P2 (mm)	5.9	5.9	5.9	5.9	5
coil space P3 (mm)	5.1	5.1	5.1	5.1	4.5
coil space P4 (mm)	3.82	3.82	3.82	3.82	4
coil space P5 (mm)	2.55	2.55	2.55	2.55	3

Fig.A1 Geometry of the test valve springs; series C, D and E.

By this method of data assembly we are able, with only eleven springs, to be able to demonstrate the characteristics of tapered springs which have either simple or compound tapers or have, or do not have, coil spring progression.

THE VALVE SPRINGS SET A (THE SIMPLE TAPER): A0, A0.1, A0.2, A0.3

In Fig.A1 is a table giving the physical dimensions of all of the valve springs. The valve springs are labelled in sets. The first set is A0 to A0.3. The springs are drawn in CAD, are modelled in 4stHEAD, and are presented in Figs.A2 to A5. At the left on each Figure is the CAD drawing of the spring, in the middle is the 4stHEAD model of the spring at zero deflection and at the right is the 4stHEAD model of most springs at 17 mm deflection; spring A0 is an exception, for reasons to be explained below, at 19 mm deflection. Clearly, the central and left images of the form, spacing and profile of the helix should be 'identical'.

The springs A0 to A0.3 are simple tapered springs with a 'perfect' equal coil spacing as defined for a 'perfect' parallel spring. Actually, spring A0 is precisely that as its side spaces D1 to D7 are all zero. The side spaces D1 to D7 for springs A0.1 to A0.3 are, as their label suggests, tapered by 0.1 to 0.3 mm per coil so that spring A0.3 is the most tapered of the set. The A spring set are very similar in design concept to the JW and GM springs presented in Paper Two in that their spring tapers D are not particularly pronounced and their coil spaces P are roughly equal; see Figs.2.5 and 2.7. The more pronounced taper of spring A0.3 in Fig.A5, compared to spring A0 (no taper) in Fig.A2, or spring A0.1 (minimum taper) in Fig.A3, is reasonably obvious although it is more visually apparent from the 4stHEAD model 'wire-frame' helix than the CAD drawing.

Red or blue coloured elements in the 4stHEAD graphics of spring deflection under load, see Fig.1.11 and its related discussion, denote

bound or trapped spring elements which raise the stiffness of the spring. Hence, at 17 mm spring deflection in Figs.A4 and A5, the red coloured helix elements signify progression because some stiffening of the spring has occurred prior to full spring deflection.

In Figs.A6 to A9 are the spring characteristics of the A0, A0.1, A0.2, and A0.3 springs for load, stiffness, natural frequency and shear stress, respectively. The shear stress is the maximum value encountered at any element on any coil at any given spring deflection and 1250 MPa is conventionally regarded as the maximum safe design limit value assuming that

(a) reasonable racing durability is required and (b) high quality Cr-Si wire is used in their manufacture.

In Fig.A6 the load carrying capacity of the springs is seen to increase from the zero taper A0 spring to the maximum taper A0.3 spring; this harks back to the mathematics of Fig.1.10 and its related discussion where the lesser is any spring coil diameter then the lesser is the

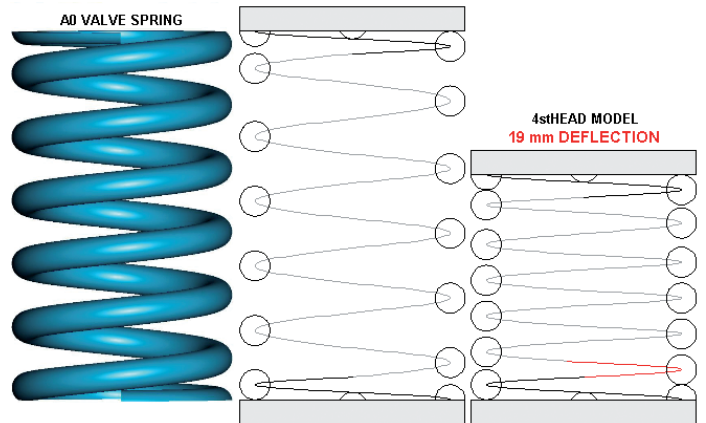


Fig.A2 CAD drawing and 4stHEAD models of the A0 valve spring.

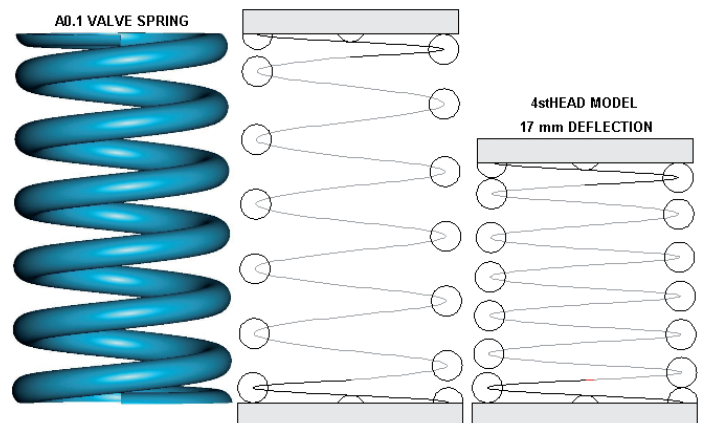


Fig.A3 CAD drawing and 4stHEAD models of the A0.1 valve spring.

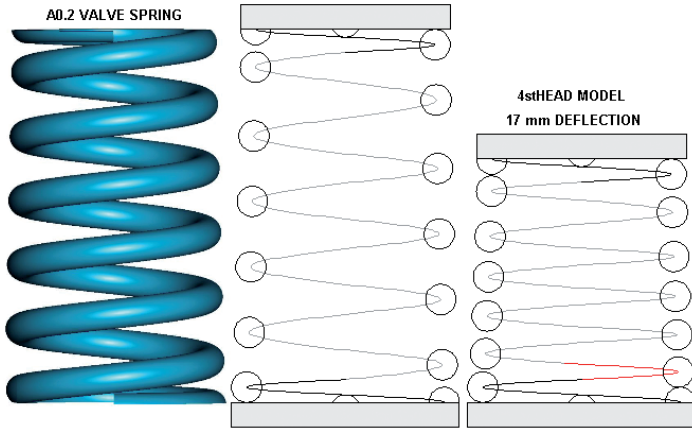


Fig.A4 CAD drawing and 4stHEAD models of the A0.2 valve spring.

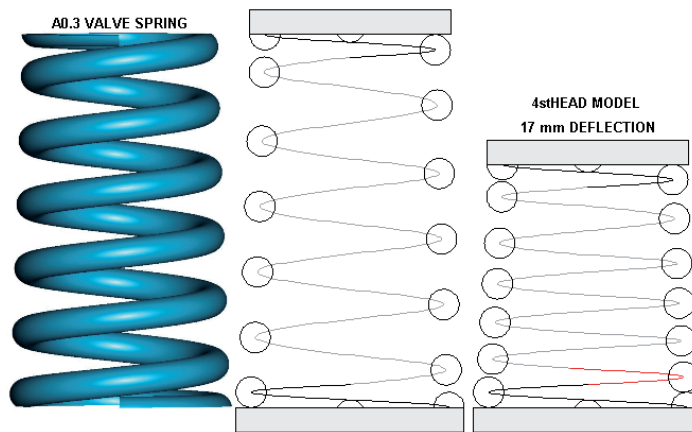


Fig.A5 CAD drawing and 4stHEAD models of the A0.3 valve spring.

deflection under a given load. By definition, less deflection at equal load means a stiffer spring, see Fig.A7 and, as forecast in Paper One, the higher natural vibration frequencies seen in Fig.A8.

Perhaps it is not so obvious why, in Fig.A7, the increasing taper of the springs from A0 (none) to A0.3 exhibits rising progression, i.e., the spring stiffness jumps as coil elements bind ever earlier with spring deflection. On all tapered springs, the bottom coil has the largest radius and hence that coil is weaker than an upper (lesser radius) coil. At any given load on the tapered spring, the top coil will deflect the least and the bottom coil the most. Therefore, at equal levels of spring deflection in Fig.A6 the most tapered of the spring set carries the highest load. This means that its bottom coils are the most compressed of any and ultimately bind ever earlier on the dead coil. For the A0.1 spring, the numeric data output from 4stHEAD predicts that this occurs at 17.51 mm deflection for the A0.1 spring, for the A0.2 spring at 16.79 mm, and for the A0.3 spring at 15.675 mm; this explains why we have chosen to show the 4stHEAD model at 17 mm deflection in Figs.A3 to A5.

The more eagle-eyed among our readership will now doubtless ask why the A0 spring, which has no taper, exhibits progression at 18.79 mm deflection. In Fig.A7, at the right, is the 4stHEAD model of the A0 spring at 19 mm deflection; the red colour of the helix indicates that some 50% of this active coil is bound. Due to the helix profile of the bottom active coil and that of the bottom dead coil, even in a parallel spring there comes a point approaching maximum deflection where some elements of this active coil will inevitably bind on the dead coil and so the stiffness rises. This effect was seen and discussed earlier

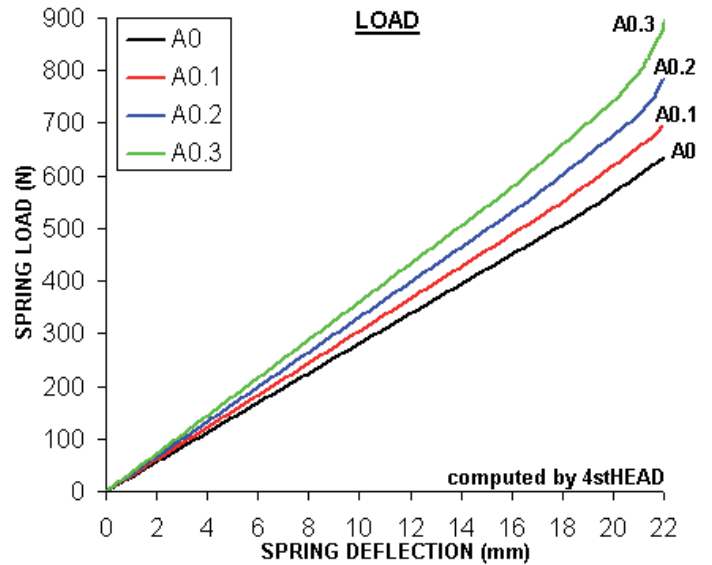


Fig.A6 Load carrying characteristics of the A set of valve springs.

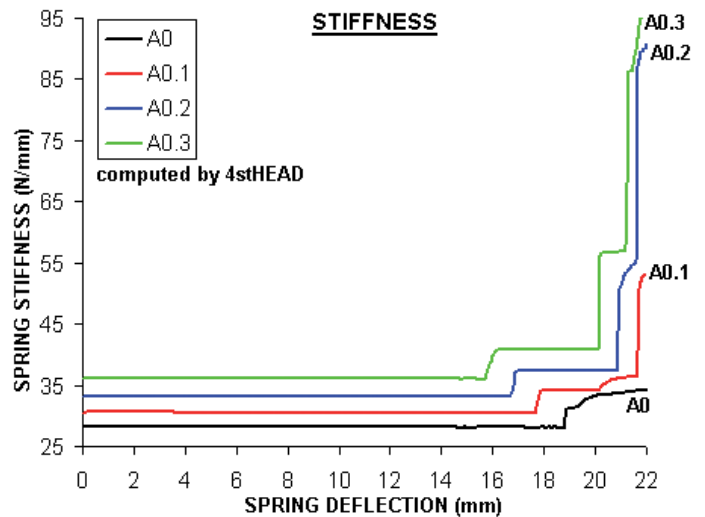


Fig.A7 Stiffness characteristics of the A set of valve springs.

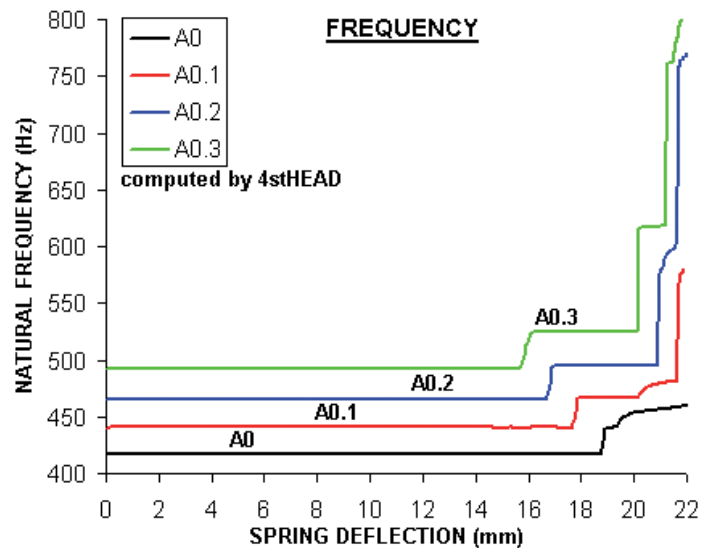


Fig.A8 Vibration characteristics of the A set of valve springs.

with respect to Fig.1.17 and is commonly observed experimentally for plain parallel springs with (supposedly) no coil space progression.

Actually, there is a second, perhaps even more interesting, phenomenon for the A0 data shown in Fig.A7, as the spring stiffness

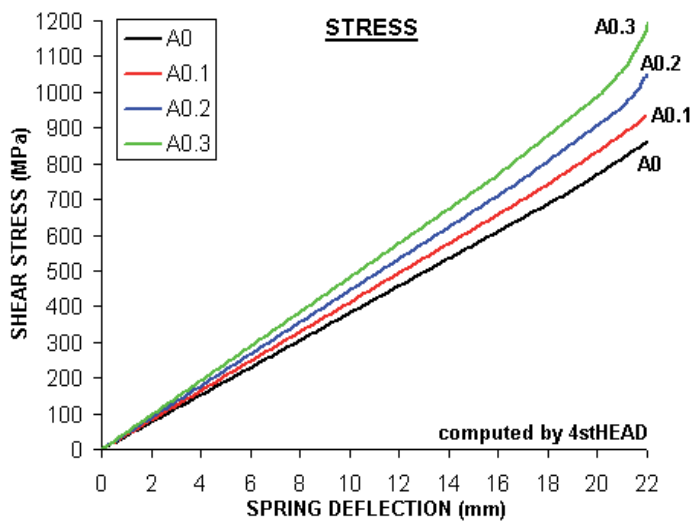


Fig.A9 Shear stress characteristics of the A set of valve springs.

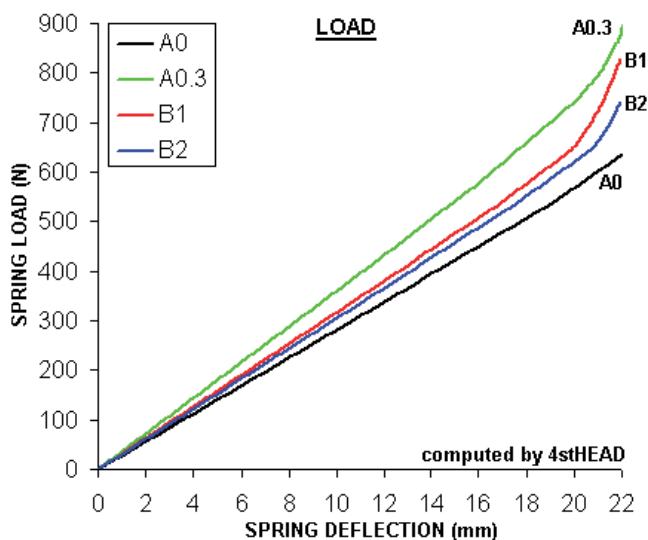


Fig.A12 Load carrying characteristics of the B set of valve springs.

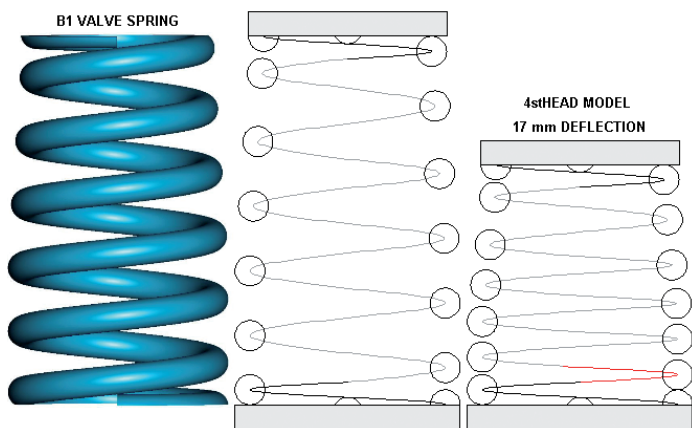


Fig.A10 CAD drawing and 4stHEAD models of the B1 valve spring.

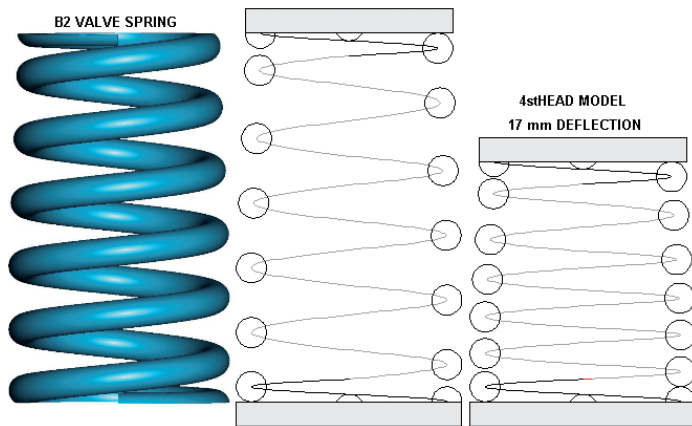


Fig.A11 CAD drawing and 4stHEAD models of the B2 valve spring.

surprisingly falls from 28.19 N/mm at 0.2 mm deflection to 28.07 N/mm at 18.69 mm, i.e., the computation increment just before the coil stiffness jumps. This decrease of stiffness is so small that it barely registers in Fig.A7; it is due to the application of the equation seen in Fig.1.10 where, as any spring deflects incrementally, the helix angle (α) of all of the spring elements decreases, the $\cos^2\alpha$ term rises towards unity, the $\sin^2\alpha$ term tends to zero, the deflection (d) increases, and the spring stiffness consequently reduces.

In Fig.A8 is presented the natural frequency characteristics for the A set of springs. As the published equation from Paper One would dictate, the higher the stiffness so too is normally the natural frequency [A2]. The shift from A0 to A0.3 is about 75 Hz upwards from 417 Hz or about 6%.

From the designer's viewpoint the load and stiffness graphs predicted by 4stHEAD would rank as a high priority in the process of

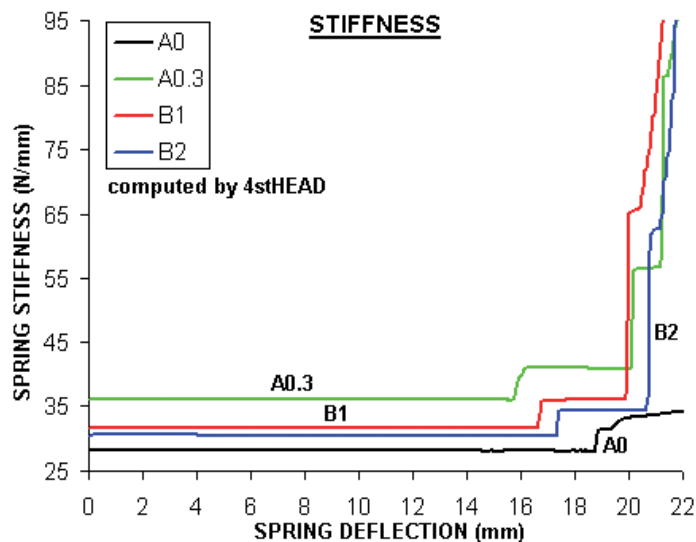


Fig.A13 Stiffness characteristics of the B set of valve springs.

optimising any given valve spring for its application. In this context, the Fig.A9 is equally important as it exhibits the shear stress for the A spring set. Unsurprisingly, as the spring coils of A0.3 can carry the highest load so too they must suffer the greatest stress in the wire. The difference from a safe maximum of 862 MPa for A0, to 1195 MPa for A0.3 is considerable; the latter stress of 1195 MPa for spring A0.3 is also uncomfortably close to the assumed safe maximum value of 1250 MPa. We rather doubt that even the most experienced designer could intuitively look at the springs in Figs.A2 to A5 and be aware that the shear stress in the wire could have this degree of variability ranging from 'very safe' to 'potential failure'.

In Fig.A7, the rapid rise of stiffness for all of the springs at about 21 mm deflection indicates that the spring is almost completely coil bound. The designer would probably decide that a nominal 19 mm deflection could be safely tolerated, giving rise to, say, a valve lift of 13 mm and a preload of 6 mm; within 4stHEAD that presumption could be checked dynamically for the entire valvetrain with the click of a mouse. The ensuing dynamic analysis would reveal if there is any potential at the design engine speed for an inertial surge around maximum valve lift of the coil spring elements which could induce full compression of the lower spring coils. If this happened to, say, the A0.3 spring, that would trigger the shear stress to reach the 'potential failure' mode of 1195 MPa even though its stress at the nominal 19 mm 'design' deflection is predicted to be a 'safe' 933.5 MPa [A1].

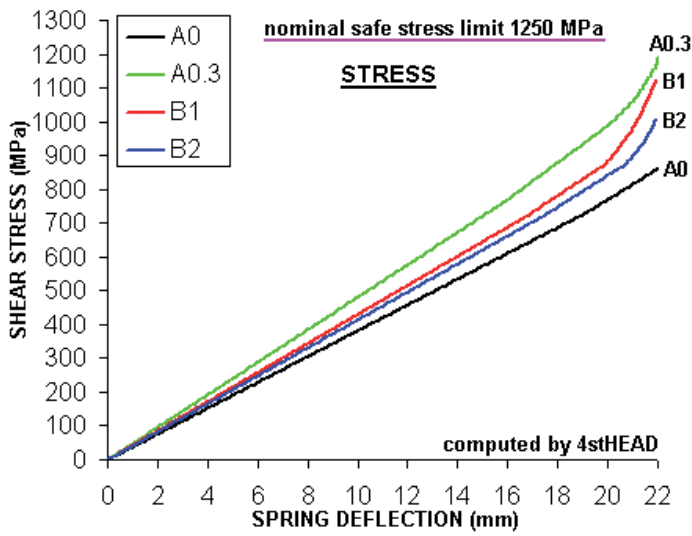


Fig.A14 Shear stress characteristics of the B set of valve springs.

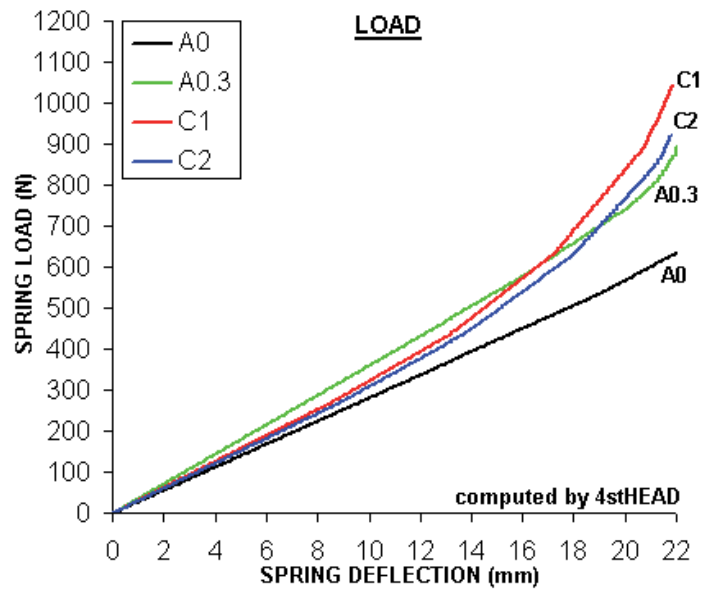


Fig.A17 Load carrying characteristics of the C set of valve springs.

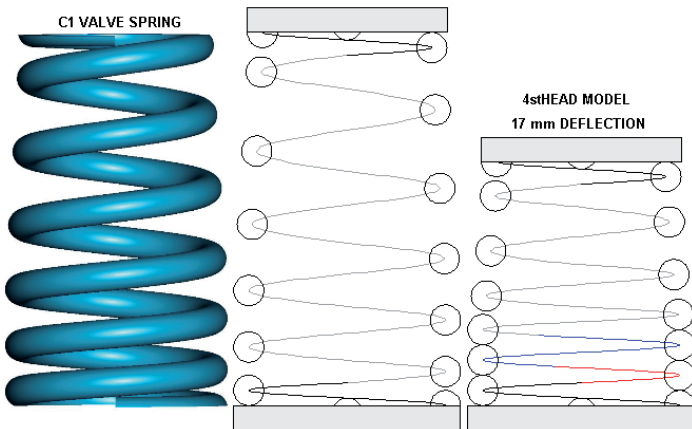


Fig.A15 CAD drawing and 4stHEAD models of the C1 valve spring.

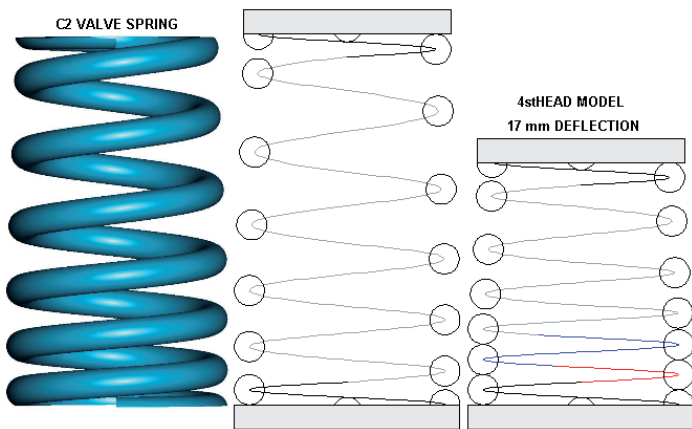


Fig.A16 CAD drawing and 4stHEAD models of the C2 valve spring.

THE VALVE SPRINGS SET B (THE TWO-STAGE TAPER): B1, B2

In the table that is Fig.A1 are the dimensions of the B springs. For the B1 and B2 springs, there is taper only on the top three coils of 0.6 mm/coil and 0.4 mm/coil, respectively, giving rise to a top coil diameter of 26.4 and 28.6 mm, respectively, which top coil diameters are the same as springs A0.3 and A0.2, respectively. There is no progression on the coil spaces P of the B springs; in that respect they are identical to the A springs. They are shown in Figs.A10 and A11 in the same manner as for the A springs in Figs.A3 to A5. Their profile is not dissimilar to the SS spring in Paper 2 [A3], i.e., the bottom half coils are parallel and the spring taper is concentrated at the top.

The load, stiffness and stress characteristics predicted for the B

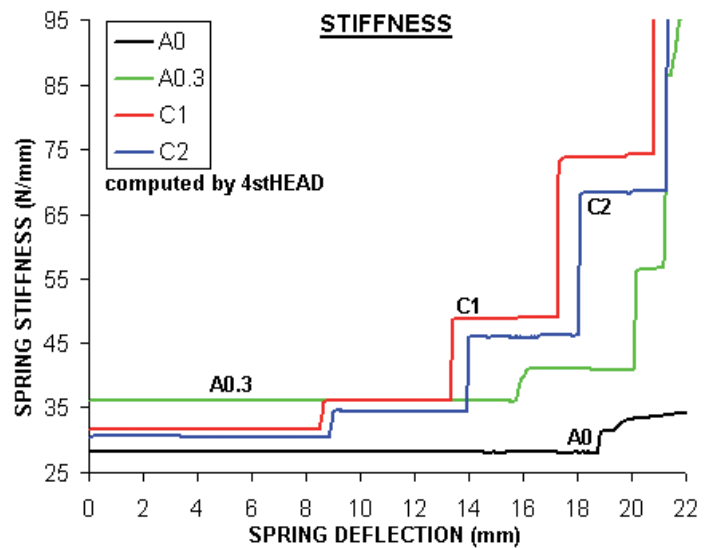


Fig.A18 Stiffness characteristics of the C set of valve springs.

springs are illustrated in Figs.A12, A13, and A14, respectively. As the characteristics for the A0 and the A0.3 baseline springs are drawn on these same Figures, it can be seen that the characteristics for the B set springs lie between them. Considering that the bottom half of both B set springs are identical to the A0 spring with no taper, and that the top diameter of the B1 coil is the same as the A0.3 spring, that the spring characteristics of the B springs are bracketed by the A springs cannot come as a numerical surprise.

THE VALVE SPRINGS SET C (TWO-STAGE TAPER WITH PROGRESSION): C1, C2

In the table of Fig.A1 are the dimensions of the C springs. The C springs have the two-stage taper of the B springs but introduce progression of the spring by decreasing the coil spaces P towards the bottom of the spring; the progression of each C spring is identical. They are shown in Figs.A15 and A16 in the same manner as for the B springs in Figs.A10 to A11. The load, stiffness and stress characteristics predicted for the C springs are illustrated in Figs.A17, A18, and A19, respectively, together with the benchmark A0 and A0.3 springs.

The load and stiffness behaviour of the C springs exceed those of the A or B springs. Clearly, the introduction of spring progression is the reason as the two-stage taper profiles of the C springs are the same as for the B springs. On Figs.A15 and A16, it can be observed that many

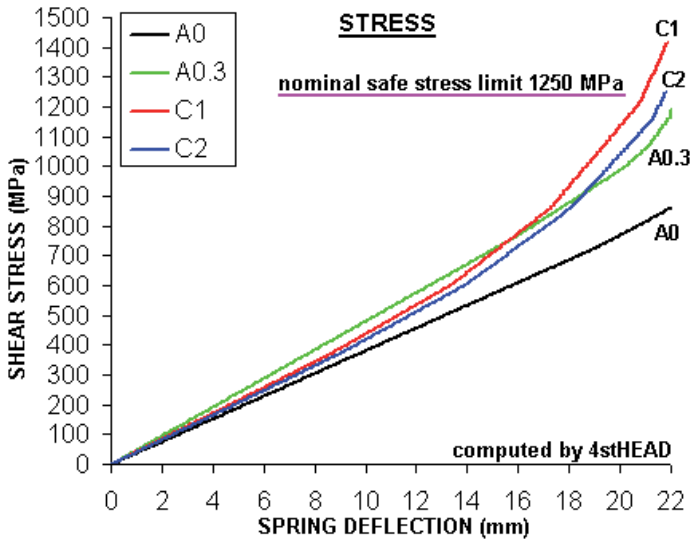


Fig.A19 Shear stress characteristics of the C set of valve springs.

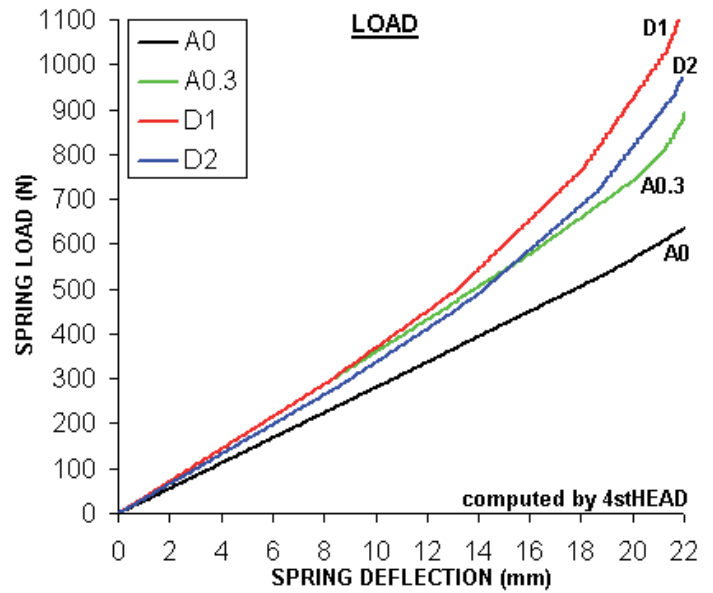


Fig.A22 Load carrying characteristics of the D set of valve springs.

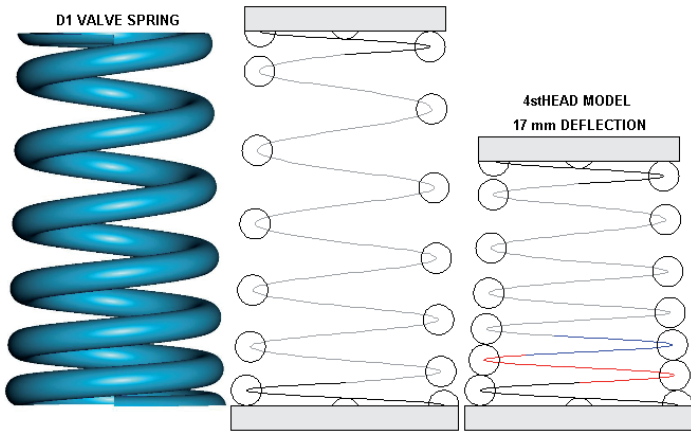


Fig.A20 CAD drawing and 4stHEAD models of the D1 valve spring.

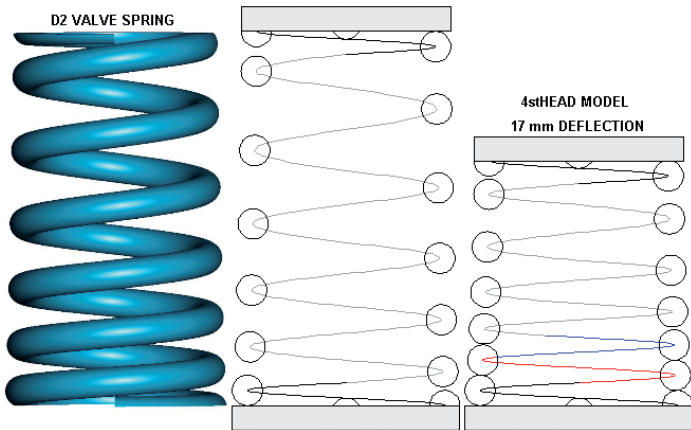


Fig.A21 CAD drawing and 4stHEAD models of the D2 valve spring.

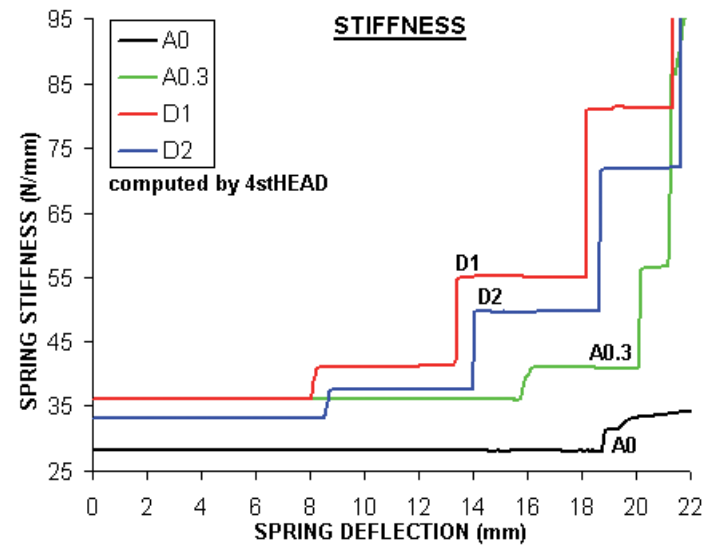


Fig.A23 Stiffness characteristics of the D set of valve springs.

more coil elements have become bound at 17 mm deflection (red and blue trapped elements) by comparison with Fig.A10 (red only) and Fig. A11 (none trapped). That the C springs have higher stiffness levels, and certainly at 17 mm deflection, can be seen in Fig.A18.

In Fig.A17, the maximum load carried by the C springs exceeds that of the A0.3 spring, yet at 10 mm deflection it is less than it. In Fig. A18, we can see that the starting stiffness of the C springs (up to 9 mm deflection) are less than the A0.3 spring, they equal it from 9 to 14 mm, and only exceed it from there to maximum deflection. This is precisely the design ethos behind the use of spring progression; we only require

the higher loads and increased spring stiffness around maximum valve lift where inertia of the valve and its associated follower mass will attempt to loft, causing valvetrain component separation with significant dynamic stresses. Valve spring progression provides those desirable characteristics while, as shown in Fig.A17, the spring load at lower spring deflections can be reduced thereby decreasing the cam-to-tappet and other valvetrain component contact forces. The desirable upshot is that the friction power to drive them and the wear upon them is reduced. To be effective as a progressive spring in the manner indicated, the spring stiffness should start to increase at about 50% of maximum deflection; the C springs do that but the A and B springs do not. It is interesting to note that in Paper Two the JW and GM springs fail by this same criterion but the SS spring would meet it.

Everything comes at a price, as the designer finds in Fig.A19. The maximum shear stress on the C2 spring is 1249.4 MPa and for the C1 spring it is 1416 MPa. This outcome renders the C spring design unacceptable even at the static design stage because it is almost inevitable that any dynamic design will reveal high maximum stress levels on some spring coils at lesser deflections.

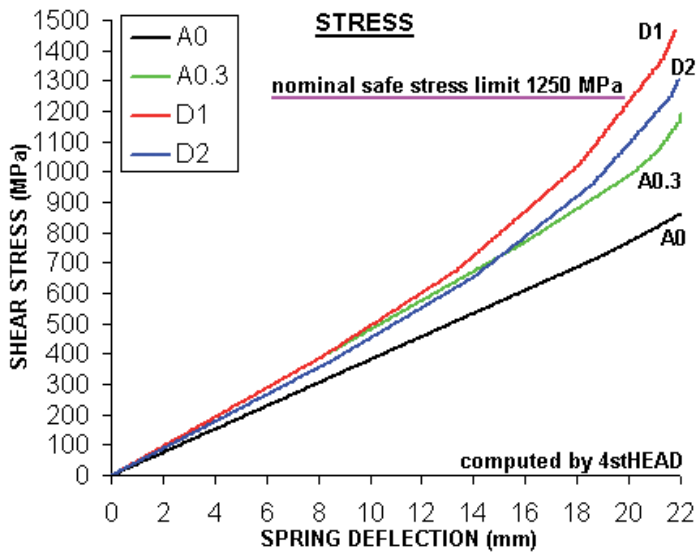


Fig.A24 Shear stress characteristics of the D set of valve springs.

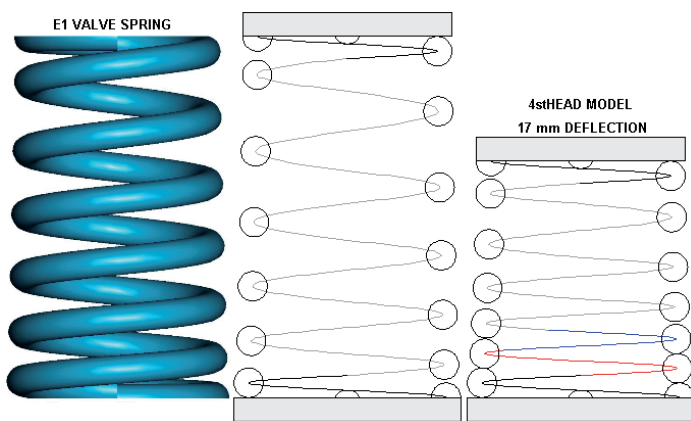


Fig.A25 CAD drawing and 4stHEAD models of the E1 valve spring.

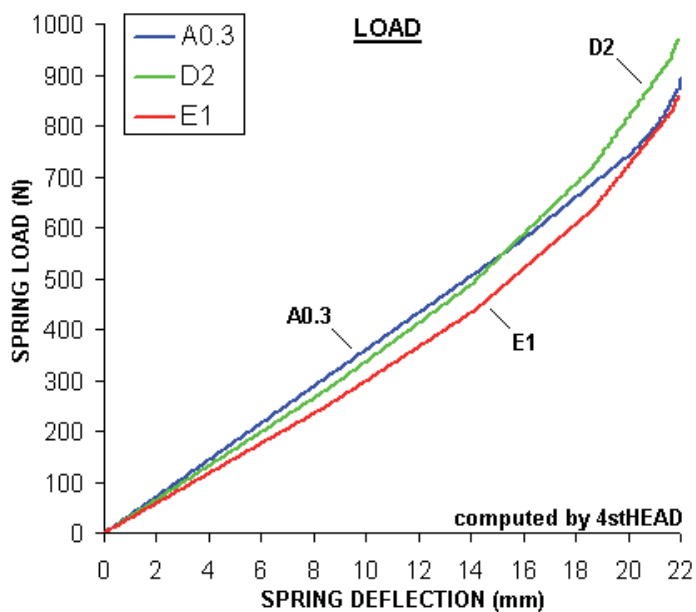


Fig.A26 Load carrying characteristics of the E1 valve spring.

THE VALVE SPRINGS SET D (SINGLE TAPER WITH PROGRESSION): D1, D2

In the table of Fig.A1 are the dimensions of the D springs. The D1 and D2 springs have the single taper of the A0.3 and A0.2 springs, respectively, but the progression of each D spring is the same as

for a C spring. The design aim is to achieve the more desirable characteristics of the C springs without raising the shear stress to an unacceptable level.

The D springs are shown in Figs.A20 and A21 in the same manner as for the C springs in Figs.A15 to A16. The load, stiffness and stress characteristics predicted for the D springs are illustrated in Figs.A22, A23, and A24, respectively, together with the benchmark A0 and A0.3 springs.

From an examination of the Figs.A22, A23, and A24, it becomes clear that your authors just failed the 'intuitive designer' test because the load and stiffness levels of the D springs are higher than the C springs and the maximum shear stress of the D1 and D2 springs are 1486 MPa and 1303 MPa, respectively; i.e., greater than the C1 and C2 springs and equally unacceptable.

What to do? Your authors riposte to this 'failure' is spring E1.

THE VALVE SPRING E1 (SINGLE TAPER WITH PROGRESSION): E1

In the table of Fig.A1 are the dimensions of the E1 spring. The E1 spring has the single taper of the D2 or A0.2 springs and the progression of the E1 spring is almost identical to each D or C spring, but is subtly different. Then, the outside diameter (Ds) of the E1 spring is made 1 mm greater than that the A, B, C or D springs, which were identical at 30 mm. To reiterate, the design aim for the E1 spring is to achieve the more desirable characteristics of the C springs without raising the shear stress to their unacceptable level.

The E1 spring geometry is shown in Fig.A25 in the same manner as for the other springs. The load, stiffness and stress characteristics predicted for the E1 spring are given in Figs.A26, A27, and A28, respectively, together with the benchmark A0.3 spring and the D2 spring, from which design the spring E1 is evolved with fairly minor geometrical changes. The authors did a better design job this time as the maximum shear stress for the A0.3, D2, and E1 springs are 1195, 1303 and 1185 MPa, respectively. The E1 design in this regard is acceptable, if 'marginal'.

The main design success is the reduction of valvetrain friction at about 50% deflection, where spring progression begins. The spring loads at 13 mm deflection for the A0.3, D2, and E1 springs are 470, 450 and 400 N, respectively. For the E1 progressive spring this potentially represents a drop in parasitic friction loss of 13% over the non-progressive A0.3 design.

Yet another design criterion is also met, as the spring loads at maximum deflection for the A0.3 and E1 springs are virtually identical at 874 and 860 N, respectively, so their ability to control component separation and valve lofting would be very similar. The designers of the JW and GM springs should perhaps take note.

GENERAL CONCLUSIONS WITH RESPECT TO TAPERED SPRING DESIGN

One of the reasons postulated for the use of tapered springs is that one can use a single valve spring which, being tapered and 'lighter' than its parallel equivalent, so shed valve spring mass from the valvetrain design. If one is replacing a double spring design with a single tapered spring it is more than likely that the maximum load capacity of the

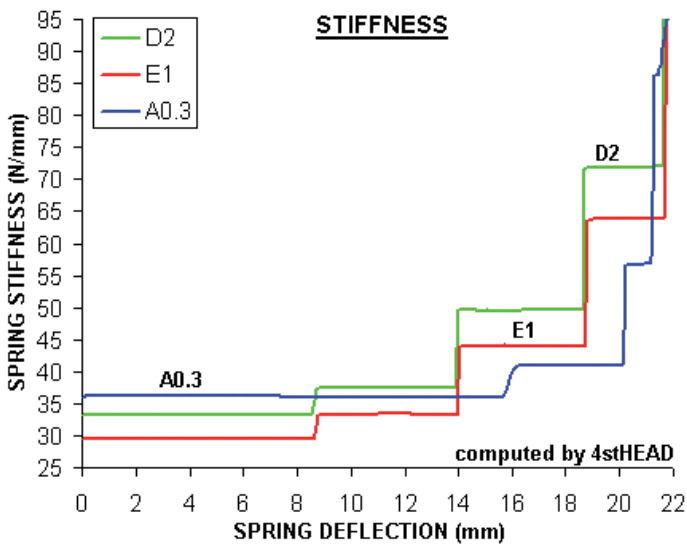


Fig.A27 Stiffness characteristics of the E1 valve spring.

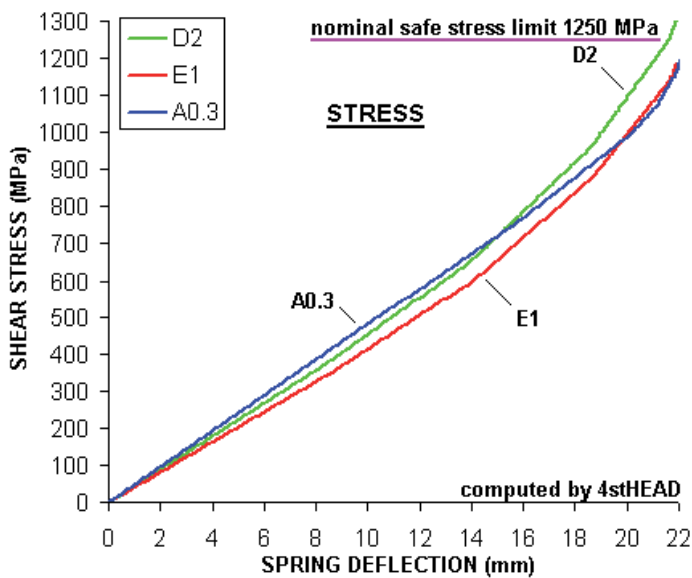


Fig.A28 Shear stress characteristics of the E1 valve spring.

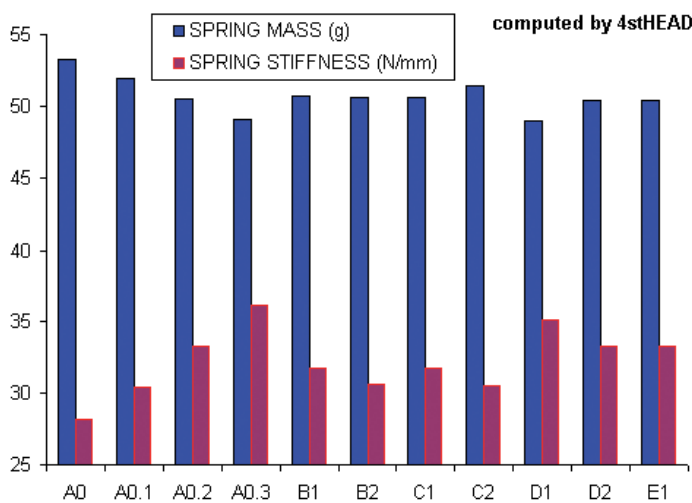


Fig.A29 Table of computed mass and stiffness of the test springs.

single tapered spring must be approximately equal to the total of the two spring combination it replaces.

If one graphs the computed valve spring mass and stiffness, tabulated in Fig.A1, and presents it in Fig.A29, it becomes clear that for the A spring set (A0 to A0.3) the spring mass does decrease and the stiffness and the load capacity does rise. For the other spring sets B, C and D, the spring mass varies very little and would be approximately

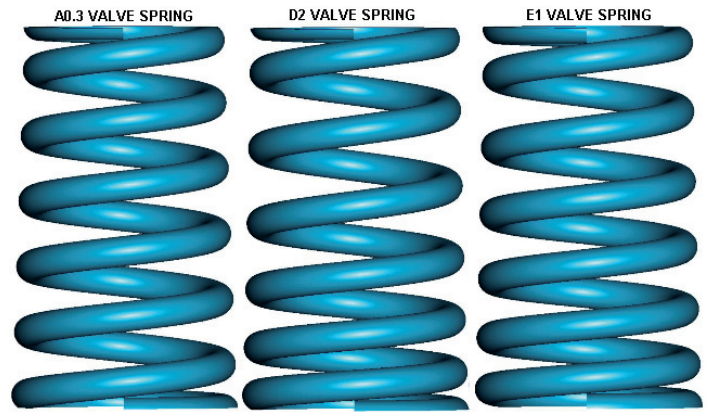


Fig.A30 The CAD drawings of the A0.3, D2 and E1 valve springs.

equal to spring A0.2.

As spring progression is introduced, in the C and D springs, while the load carrying capacity of the tapered spring does increase it does so at the expense of high, and potentially unacceptable, shear stresses. Hence, the design of a single tapered spring layout becomes a balancing act between the required load carrying capacity to prevent valve lofting under dynamic conditions and the maximum shear stress that can be tolerated for the wire.

The design changes to the geometry of the spring to accomplish this are subtle, as can be seen from our final demonstration springs A0.3, D2 and E1, shown in Fig.A30. If it was not for the label atop each spring, we could almost defy our readers to tell which was which in a 'blind' test. As the design changes to the geometry of the spring, in order to optimise it, are subtle, many such computations are required. In that situation, a FEA model that takes much longer to complete a computation by comparison with the 4stHEAD type of model, requires the designer to be very, perhaps unnecessarily, patient.

GENERAL CONCLUSIONS

It is possible today to theoretically model the load, stiffness, natural frequency, and stress characteristics of all types of helical springs that are typically used in engine valvetrains, not only with some reasonable degree of accuracy but also reasonably quickly on a desktop PC, using software [1.4]. If software is proposed for such a purpose, experimental proof must be presented of its accuracy to model all types of valve spring for their spring characteristics. Without such proof, a theoretical design procedure must be suspect as a viable design tool. With such proof, the theoretical design procedure can be reliably employed to give some design guidance where none has previously existed; to wit, this Appendix.

REFERENCES

[A1] 4stHEAD Valvetrain Analysis updates December 2008 and January 2009, text and avi, www.profbclairandassociates.com.

[A2] G.P. Blair, C.D. McCartan, W.M. Cahoon, "Valve Spring Design Paper 1", Paper 1 of 3 Papers, Race Engine Technology, Volume 7, Issue 1, January 2009. Available as download at www.profbclairandassociates.com, January 2009.

[A3] G.P. Blair, C.D. McCartan, W.M. Cahoon, "Valve Spring Design Paper 2", Paper 2 of 3 Papers, Race Engine Technology, Volume 7, Issue 2, February 2009. Available as download at www.profbclairandassociates.com, February 2009.